Novel simulation of composite material behavior subjected to hyper-velocity impact (HVI) and produced secondary debris by using smoothed-particle hydrodynamics code (SPH) methodology in LS-DYNA

Efthimios Giannaros[1], Athanasios Kotzakolios[1], Stavros Tsantzalis[1], Vassilis Kostopoulos[1]*, Gianni Campoli[2]

[1]Applied Mechanics Laboratory, University of Patras, Greece.

[2] European Space Agency ESA/ESTEC, The Netherlands.

*corresponding author, kostopoulos@mech.upatras.gr

1 Abstract

Present paper deals with the simulation of hypervelocity impact response of composite fiber reinforced polymer material (CFRP) and produced secondary debris using SPH methodology in LS-DYNA. A novel verification procedure for modeling of composite laminate to hyper-velocity impact loading using SPH methodology is proposed. The investigation starts with four baseline static tests whose results are compared with theoretical ones in order to ensure the efficiency of the hydrodynamic code to quasi-static level. Afterwards, published HVI experimental tests to CFRP laminates are numerically reproduced whereas the numerical and the experimental ballistic limit, crater diameter as well as the secondary debris distribution are correlated.

2 Introduction

The escalating usage of composite materials to improve fuel efficiency while reducing the structural mass of satellites and manned spacecrafts has become high priority target to the space industry. On the other hand, high moving space fragments such as old satellites, spent rocket stages and fragments from collision can devastate the composite structures producing thousand fragments known as secondary debris. Therefore, the prediction of impact behavior of composites and the distribution of ejecta using high-technology simulation tools are essential and vital since the experimental investigations on this field is extremely limited due to the difficulty of tests.
The classical simulation technique implementing finite elements constitutes a robust numerical method for various static and dynamic problems; however its major drawback is the difficulty to handle the large displacements in fast-transient dynamics problems and the inability to simulate the secondary debris distribution. In past, several studies for isotropic materials impact behavior using the meshless SPH methodology of LS-DYNA code have been presented, nevertheless, the simulation of composite material behavior subjected to hyper-velocity impact using SPH in LS-DYNA is missing from the literature.

3 SPH basics

Smooth Particle Hydrodynamics (SPH) is a meshless Lagrangian method for solving partial differential equations. Essentially, in the finite element analysis the domain is discretized into elements whereas in case of SPH, it is divided into particles. In order to interpolate field variables, instead of a grid and shape functions, a kernel function is used. The value of a function f(x), at a location x, is represented by an integral form of the product of the function and a weighting factor W(r,h) (kernel function) [1], [2], [3]. The most known kernel function is the cubic B-spline function:

$$W(r,h) = \frac{C}{h^d} \times (1 - \frac{3}{2}u^2 + \frac{3}{4}u^3) \text{ for } |u| = \frac{r}{h} \le 1 \quad (1a)$$

$$W(r,h) = \frac{C}{h^d} \times \frac{1}{4}\left(2-u\right)^3 \qquad \text{for } 1 \le |u| = \frac{r}{h} \le 2 \tag{1b}$$

$$W(r,h) = 0 \qquad \text{for } 2 \le |u| = \frac{r}{h} \tag{1c}$$

Where d is the number of space dimensions, h is the co-called smoothing length which varies in time and in space, r is the distance between particles i,j and C is a constant of normalization that depends on the number of space dimensions. The Fig.1 presents the domain of integration and the kernel function shape for particle i.

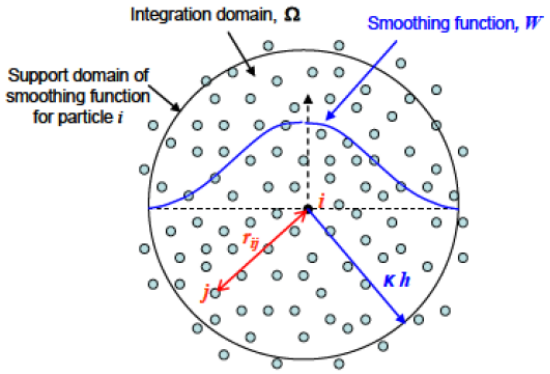

Fig.1: Domain of integration and kernel function shape for a particle.

Various geometrical and mathematical parameters affect the results of SPH models. This study was emphasized to the following parameters of SPH method which are defined into ***CONTROL_SPH**, ***SECTION_SPH** and ***DEFINE_SPH_TO_SPH_COUPLING** keyword [1], [2]:

1. Initial smoothing length h_0 and CLSH parameter
2. FORM parameter
3. CONT option
4. Penalty scale factor PFACT
5. INI parameter

3.1 Smoothing length

Smoothing length is the major geometrical parameter which defines the interaction range between particles. If the smoothing length is set to remain constant the separation between them may become so large that the particles will no longer interact with each other; on the other side, the separation may be too small significantly slowing down the simulation. The initial value of smoothing length h_0 is computed by taking the maximum of the minimum distance between every particle and multiplying it with CLSH parameter (h_0=CLSH*Initial particle distance). LS-DYNA provides the capability of variable smoothing length using Hmin and Hmax scale factors. The smoothing length increases when particles separate from each other and reduces when the concentration of particles is important. It varies to keep the same number of particles in the neighbourhood [1], [2]. In this study, regular distribution of particles was adopted for the elimination of inconsistencies due to the incompleteness of kernel function.

3.2 CLSH parameter

CLSH parameter works as scale factor in smoothing length. The higher the CLSH parameter is, the more extensive the influence of kernel function is. The CLSH parameter is the only mathematical parameter for definition smoothing length during the initiation of SPH code. In current study, influence analysis was executed for different values of CLSH parameter.

3.3 FORM parameter

The FORM parameter in ***CONTROL_SPH** keyword defines the particle approximation theory. Eight different approximation theories exist in LS-DYNA. Essentially, the FORM parameter changes the equation of momentum conversation. The FORM 7 and 8 provide the total Lagrangian formulation without and with renormalization respectively. The preliminary study showed that FORM 8 provides stress consistency and excellent results in relation to theoretical and finite element results in quasi-static level. But due to the fact that Lagrangian kernel is applied using FORM 8 and therefore neighbours' list remain constant throughout the calculation [4], the large deformations in HVI

preliminary simulations lead to termination of analysis and non reasonable results. For this reason, this investigation was focused on the default formulation (FORM=0), renormalization approximation (FORM=1), symmetric formulation (FORM=2) and symmetric renormalized approximation (FORM=3). According to the LS-DYNA manual [1], [2], the following equations are applied for the above formulations:

$$\frac{dvi}{dt} = -\sum_{j \in P} mj\left(\frac{\sigma i}{\rho i^2} Aij - \frac{\sigma j}{\rho j^2} Aji\right) \quad \text{FORM=0} \tag{1}$$

$$\frac{dvi}{dt} = -\sum_{j \in P} mj\left(\frac{\sigma i}{\rho i^2} Aij - \frac{\sigma j}{\rho j^2} Aji\right) : Bij \quad \text{FORM=1} \tag{2}$$

$$\frac{dvi}{dt} = -\sum_{j \in P} mj\left(\frac{\sigma i}{\rho i^2} + \frac{\sigma j}{\rho j^2}\right) \nabla Wij \quad \text{FORM=2} \tag{3}$$

$$\frac{dvi}{dt} = -[\sum_{j \in P} mj\left(\frac{\sigma i}{\rho i^2} + \frac{\sigma j}{\rho j^2}\right) \nabla Wij] : Bij \quad \text{FORM=3} \tag{4}$$

Where j the number of particles, W is the value of kernel function, m_j is the weight of particle j, v_j the velocity components at particle i, ρ_i the density at particle i, σ_i is the stress tensor at particle i, A_{ij} is the gradient of kernel function.

3.4 CONT parameter

The CONT parameter in ***CONTROL_SPH** keyword defines the type of particle approximation between different SPH parts. The first approximation type is the standard SPH interpolation in which particles have a spatial distance (smoothing length) over which their properties are smoothed by the kernel function. To activate this option, CONT parameter in ***CONTROL_SPH** has to be set to 0, and no contacts are allowed between SPH parts. The analyses of current study showed that this approach activates the interactions Nr2, Nr3 and Nr4 presented in Fig.2. The interaction Nr2 provides consistency on displacements and their derivatives for a single part. The activation of interactions Nr3 and Nr4 ensures that the interface particles between two sequential composite layers are sticky up to corresponding failure in order to transfer out of plane shear and normal loading from layer to layer respectively.

The second interaction type is the node to node contact which is introduced on the interface of the different SPH parts. The repulsive contact force acting on particle due to contact is directly proportional to the displacement between of particles. The ***DEFINE_SPH_TO_SPH_COUPLING** keyword should be activated and CONT parameter need to be set as 1 to deactivate the interaction through standard interpolation. Choosing this type, the analyses indicated that the interaction Nr1 between the projectile and layered composite particles can be treated in a great extent if the penalty scale factor (PFACT) is calibrated. Nevertheless, the inconsistency on displacements at the interface of layers still exists (Nr3 and Nr4 interaction). The solution was achieved determining a hybrid model with both standard interpolation methodology and node to node contact algorithm between projectile and each composite layer.

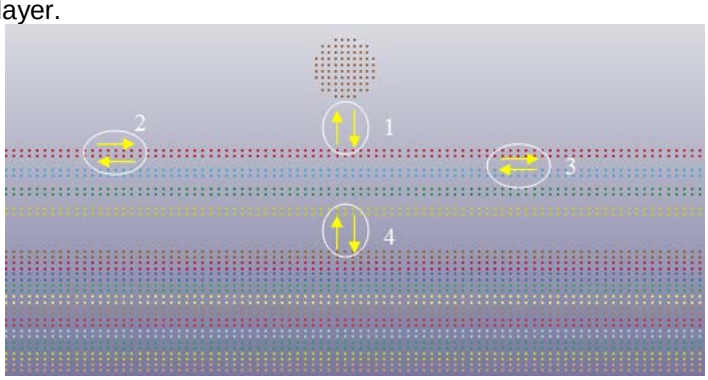

Fig.2: Treated particles interactions.

3.5 PFACT parameter

The PFACT is the main parameter for the interaction of particles through node to node contact. The penalty scale factor (PFACT) influences the spring constant of contact algorithm and therefore the contact force that is imposed on composite plate. The value of PFACT was ranged from 0.025 to 100. For small values from 0.025 to 1, the interaction between projectile and composite plate was not adequate and full penetration without interaction was presented. On the contrary, for high values (PFACT>10), very stiff interaction was computed causing projectile devastation without the expected target deformation. The most promising impact results were emerged when the PFACT was ranged from 5 to 10. For the simulations, the penalty scale factor was supposed equal to 10.

3.6 INI parameter

The neighbor search is one of the main tasks for every SPH time step. It may be a very CPU consuming task depending on the algorithm type selected. The LS-DYNA code provides three different algorithms for computation of smoothing length during the initialization. Using the global computation algorithm (INI=1), every particle is checked with the rest globally but it is a time-consuming methodology. The second and third algorithm is particle mass based algorithm (INI=0) and bucket sort algorithm (INI=2) respectively. In last algorithm, a grid of size 2h is generated and each particle is assigned to one of the boxes, then the searching for each particle starts checking other within its own and neighboring boxes as illustrated below. Due to the fact no discrepancy exist between the results of mass based and bucket sort algorithm (Fig.6) and detailed information about the theory behind bucket sort algorithm is provided in LS-DYNA manual, the last searching algorithm was chosen in present study.

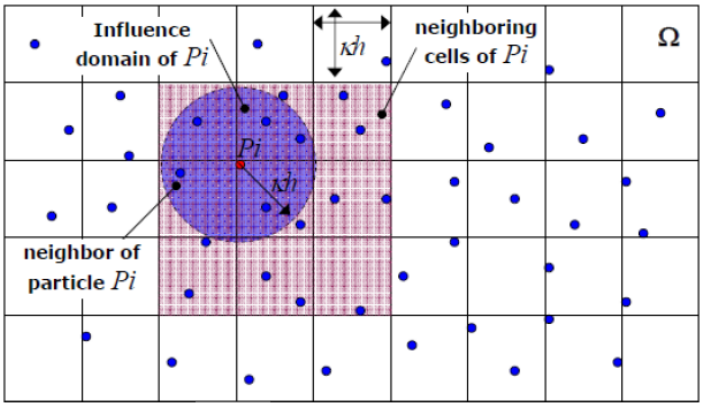

Fig.3: Bucket sort based algorithm.

4 Material models & Properties

4.1 Orthotropic material models

An investigation was performed to find composite material models compatible with SPH method implemented in LS-DYNA code. The only available orthotropic models are presented below:

- ***MAT_COMPOSITE_DAMAGE (MAT_22)**
- ***MAT_COMPOSITE_FAILURE_SPH_MODEL (MAT_59)**
- ***MAT_ORTHOTROPIC SIMPLIFIED_DAMAGE (MAT_221)**

MAT_22 uses the Chang-Chang failure criterion but it was rejected as a candidate material model due to its inability to capture longitudinal and out-of-plane compressive strength. In case of MAT_221, damage accumulation functions based on current strains, damage initiation strains and failure strains are used to reduce the elastic moduli of the composite in each of the coordinate directions in a damage mechanics approach. However, the main drawback is that the inputs consist of the complete stress/strain curve of the material in each direction which requires extensive experimental data. Therefore, the most promising candidate composite material model is MAT_59 which is explained below. It is crucial to be mentioned that none of LS-DYNA orthotropic material models can capture high strain effects when SPH methodology is applied. Additionally, these models are not capable of

representing the volumetric response (shock response) of orthotropic materials. Consecutively, the simulation of transmission of stress waves is not feasible.
MAT_59 simulates the 3-dimensional behaviour of an orthotropic composite structure. It predicts the onset of four major failure modes, namely tensile failure, transverse shear failure, compressive failure and delamination (Eq. 5-12). The occurrence of these failure modes is predicted by four independent failure criteria, based on the assumption that these failure mechanisms contribute to an ultimate failure of a composite system. Complete failure of the composites is facilitated by progressively degrading the properties of the composites [5].

4.1.1 Tensile failure

a) Longitudinal tensile failure occurs if : $\left(\frac{\sigma aa}{Xt}\right)^2+\left(\frac{\sigma ab}{Sab}\right)^2+\left(\frac{\sigma ac}{Sac}\right)^2\geq 1$, Eb, Ec $\neq 0$ (5)

b) Transverse tensile failure occurs if : $\left(\frac{\sigma bb}{Yt}\right)^2+\left(\frac{\sigma ab}{Sab}\right)^2+\left(\frac{\sigma bc}{Sbc}\right)^2\geq 1$, Ea, Ec $\neq 0$ (6)

4.1.2 Through thickness shear failure

a) Longitudinal through-thickness shear failure occurs if : $\left(\frac{\sigma aa}{Xt}\right)^2+\left(\frac{\sigma ac}{Sac}\right)^2\geq 1$, Eb, Ec $\neq 0$ (7)

b) Transverse through-thickness shear failure occurs if : $\left(\frac{\sigma bb}{Yt}\right)^2+\left(\frac{\sigma bc}{Sbc}\right)^2\geq 1$, Ea, Ec $\neq 0$ (8)

4.1.3 Delamination failure

a) Delamination occurs if the following is met: $\left(\frac{\sigma cc}{Zt}\right)^2+\left(\frac{\sigma ac}{Sac}\right)^2+\left(\frac{\sigma bc}{Sbc}\right)^2\geq 1$, Ea, Eb $\neq 0$ (9)

Where the first term is considered only if σcc>0.

4.1.4 Compressive failure

a) Longitudinal compressive failure occurs if: $\left(\frac{\sigma aa}{Xc}\right)^2\geq 1$, Eb, Ec $\neq 0$ (10)

Where σaa<0.

b) Transverse compressive failure occurs if:

$$\left(\frac{\sigma bb}{Sab+Sbc}\right)^2+\left[\left(\frac{Yc}{Sab+Sbc}\right)^2-1\right]\frac{\sigma b}{|Yc|}+\left(\frac{\sigma ab}{Sab}\right)^2+\left(\frac{\sigma bc}{Sbc}\right)^2\geq 1,\ \text{Ea, Ec}\neq 0 \quad (11)$$

Where σbb<0.

c) Through thickness compressive failure occurs if:

$$\left(\frac{\sigma cc}{Sac+Sbc}\right)^2+\left[\left(\frac{Zc}{Sac+Sbc}\right)^2-1\right]\frac{\sigma cc}{|Zc|}+\left(\frac{\sigma ac}{Sac}\right)^2+\left(\frac{\sigma bc}{Sbc}\right)^2\geq 1,\ \text{Ea, Eb}\neq 0 \quad (12)$$

Where σcc<0.

The used CFRP material type and its quasi-static properties are presented in Table 1.

General data				Stiffness Properties								
CFRP type	Density	Ply thickness	Fiber volume	E_x	E_y	E_z	v_{12}	v_{23}	v_{13}	G_{xy}	G_{yz}	G_{xz}
	g/cm^3	mm	%	GPa	GPa	GPa	-	-	-	GPa	GPa	GPa
IM600/133	1,562	0,141	55%	150	8,20	8,20	0,34	0,53	0,34	4,34	2,70	4,34
Failure Parameters (t-tension, c-compression)				**Xt**	**Yt**	**Zt**	**Xc**	**Yc**	**Zc**	**Sxy**	**Syz**	**Sxz**
				MPa	MPa	MPa	MPa	MPa	MPa	MPa	MPa	MPa
				2700	63,7	63,7	1037	235	235	140	112	140

Table 1: Quasi-static mechanical properties of IM600/133 CFRP lamina [6], [7].

4.2 Isotropic material model

In present study, the materials which was used for projectile is the aluminum AL-2017 and AL 99.5%. Therefore, the potential LS-DYNA material models that could be used to model the mechanical behavior of these materials are:

- ***MAT_PIECEWISE_LINEAR_PLASTICITY(MAT_24)**
- ***MAT_SIMPLIFIED_JOHNSON_COOK (MAT_98)**
- ***MAT_JOHNSON_COOK (MAT_15)**

According to bibliography, the most common used material model for metallic materials is Johnson-Cook as it is capable of capturing strain rate effects and temperature plasticity; also an equation of state can be included. However, MAT_98 cannot be applied when SPH methodology has been used and MAT_15 requires extensive data for its definition. Therefore, the most promising material model is MAT_24. It is an elasto-plastic material model with an arbitrary stress versus strain curve and arbitrary strain rate dependency can be defined. The failure is based on plastic strain or a minimum analysis time step size. In current study the plastic strain was adopted. The necessary variables for the definition of discussed model are 1) mass density, 2) Young's modulus, 3) Poisson's ratio, 4) Yield stress, 5) Tangent modulus and 6) Plastic strain. It is noted that the elasto-plastic behavior was treated as a bilinear stress/strain curve. The strain rate effects and volumetric response of projectile material diverges from main target of current paper and they are not examined. The quasi-static mechanical properties of projectile material are shown below.

Material	Density	Young's Modulus	Poisson's Ratio	Tensile yield strength	Ultimate tensile strength	Elongation at break
-	Kg/m3	GPa	-	MPa	MPa	-
Al 2017-T4*	2790	72	0,33	267	1400	0,65
Al 99.5%**	2712	68,9	0,33	49	157	0,272
* Properties derived by quasi-static compressive test. ** Properties derived by quasi-static tensile test.						

Table 2: Quasi-static mechanical properties of projectile material [8], [9].

5 Verification approach

The verification of SPH code and orthotropic material model MAT_59 in quasi-static level is essential and vital for the reliability of results of HVI simulations, since the stiffness and failure of composite material should be checked. The main target of this section is to investigate the influence of SPH parameters and to evaluate the validity of SPH method results compared with theoretical ones. In particular, composite laminate was examined to in-plane tensile, in-plane compressive, out-of-plane compressive and out-of-plane shear loading.

5.1 Description of model

The preliminary study showed that the model of verification procedure should be an unchanged sub-model of final SPH model which will be subjected to hypervelocity impact in order to eliminate any doubt about the reliability of results. Therefore, in current research, both the verification model and the HVI model present the same initial particles distance in all directions, material properties, lay-up and thickness. The distance of particle was kept constant at 0.1mm in X and Y directions and 0.072 mm in

Z direction. The model dimensions are 10mm (Length) x 5.2 mm (Width) x 2.21mm (total Thickness), the ply thickness was equal to 0.1437mm and 2 particles through the ply thickness were adopted. Ply-based composite modeling was used for the accurate simulation of laminate instead of homogenized based one determining the fiber orientation by vectors (AOPT=2) into keyword ***MAT_COMPOSITE_FAILURE_SPH_MODEL.** One part for each ply was generated using ***PART** keyword and 16 parts were totally created since the lay-up of composite plate is [+45/0/-45/90/90/-45/0/+45]s. The keywords ***SECTION_SPH and *CONTROL_SPH** were also defined as they include the necessary parameters of SPH code. For the interaction of particles, **CONT** parameter was set equal to zero which means that standard SPH interpolation method using kernel function was activated. Furthermore, uniform mass distribution was applied and the mass of each particle was defined using ***ELEMENT_SPH** keyword. Additionally, ***CONTROL_BULK_VISCOSITY** keyword was used to damp high frequency noise produced by shock if left unchecked. The quadratic viscosity coefficient Q1 and linear coefficient Q2 were set 1.5 and 0.5 respectively. The boundaries conditions differs for each loading cases but they were defined by the same keywords ***SPC_NODE_SET** and ***PRESCRIBED_MOTION_SET**.

5.2 In-plane tensile loading

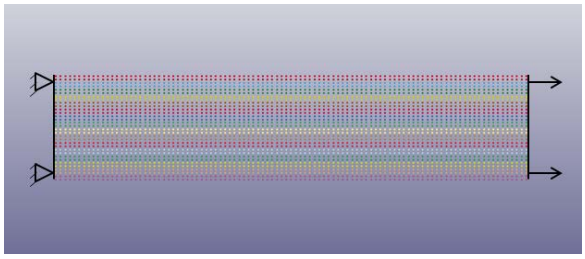

Fig.4: In-plane tension model.

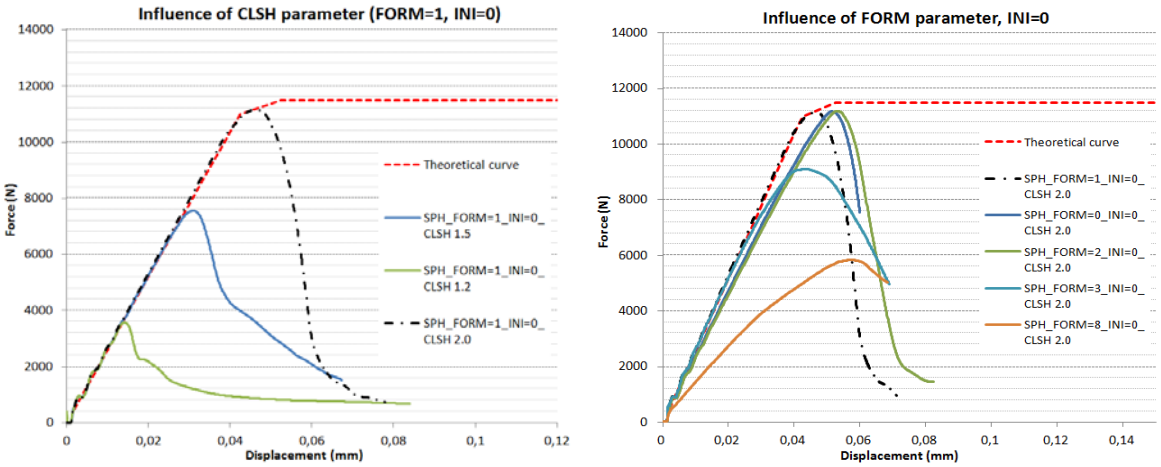

Fig.5: Influence of CLSH and FORM parameters on in-plane tensile response of composite.

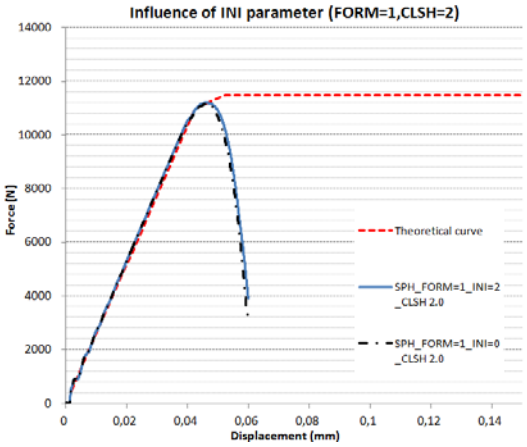

Fig.6: Influence of INI parameter on in-plane tensile response of composite.

5.3 In-plane compressive loading

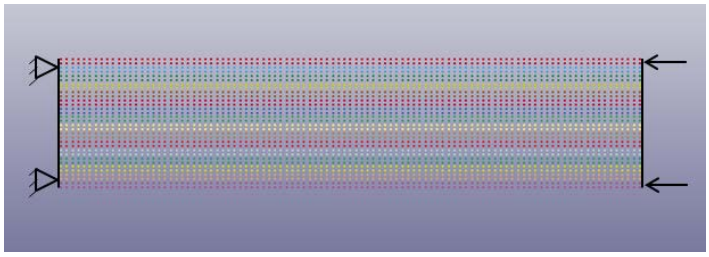

Fig.7: In-plane compression model.

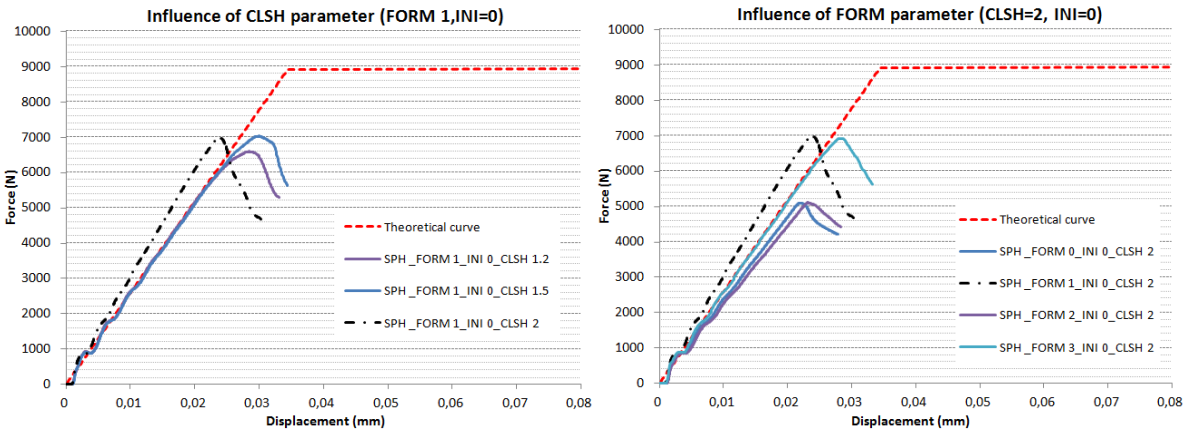

Fig.8: Influence of CLSH and FORM parameter on in-plane compressive response of composite.

5.4 Out-of-plane compressive loading

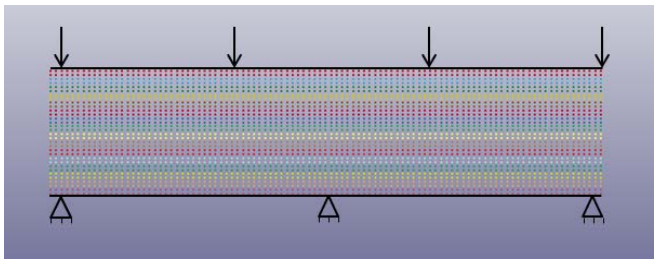

Fig.9: Out-of-plane compression model.

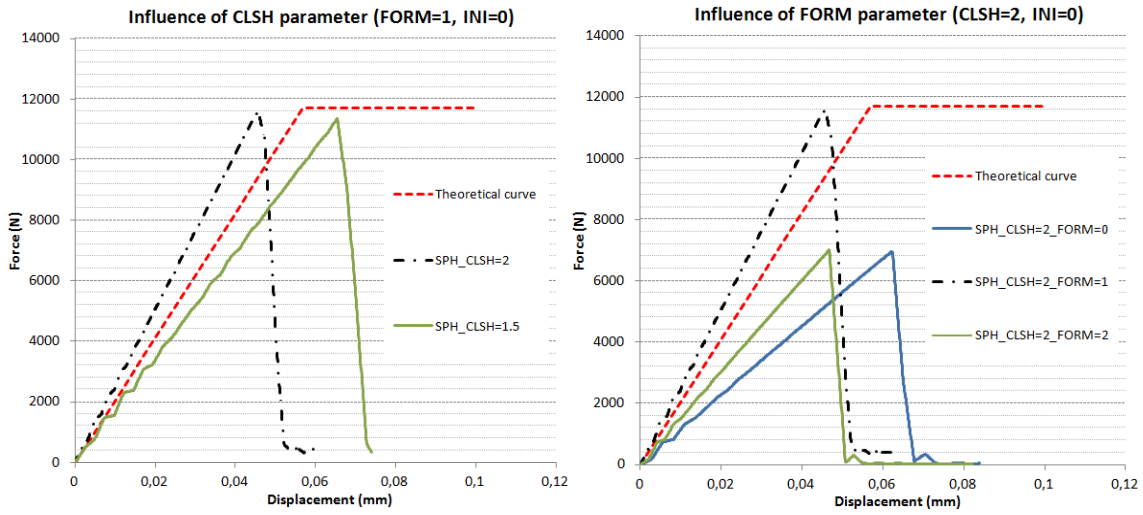

Fig.10: Influence of CLSH and FORM parameter on out-of-plane compressive response of composite.

5.5 Out-of-plane shear loading

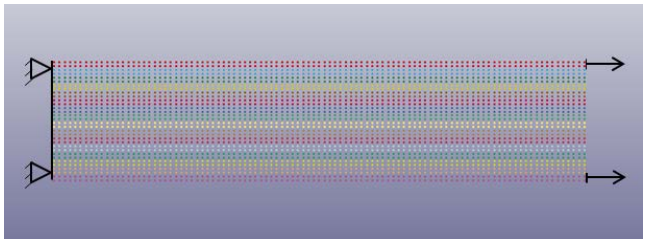

Fig.11: Out-of-plane tension model.

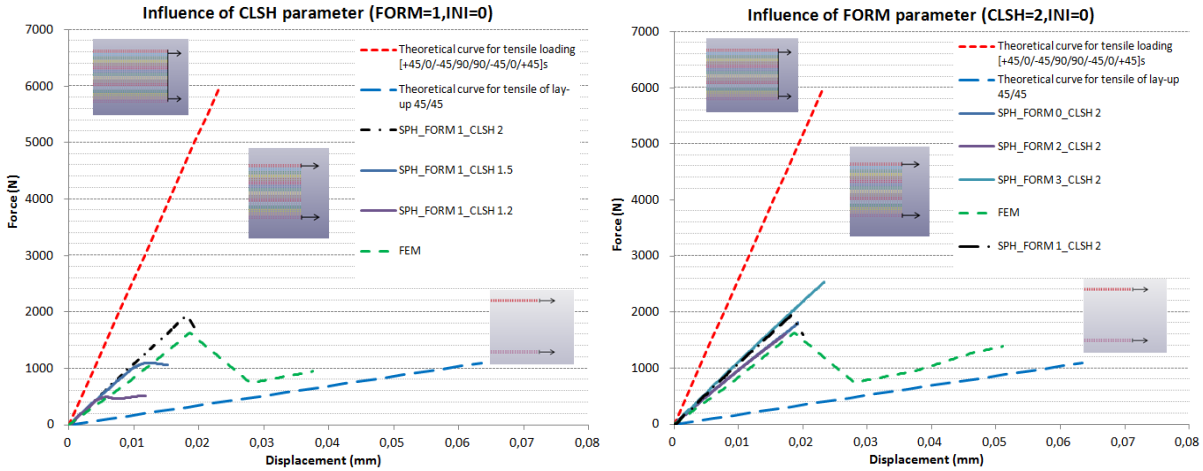

Fig.12: Influence of CLSH and FORM parameter on out-of-plane shear response of composite.

6 Hypervelocity impact simulation

6.1 Experiments

The literature experimental study [10] was chosen for the validation of SPH numerical model to hypervelocity impact. In published work [10], 45 hypervelocity impact experiments were executed on Carbon Fiber Reinforced Plastic samples (CFRP) having nominal thickness of 2.3, 3.5 and 4.3 mm. The impact tests were made with aluminium spheres of 0.8, 1.5, 1.9, 2.3 and 2.9, at velocities between 2 and 5 km/sec. The CFRP samples used in the study were made of epoxy resin (resin type 133 produced by Toho Tenax), reinforced with high-strength, medium-modulus carbon fibers (IM600 fiber type).

In current paper, four of these tests were simulated. More specifically, only the sample with 2.3mm nominal thickness and [+45/0/-45/90/90/-45/0/+45]s lay-up was modelled for 1.98 km/sec, 3.83km/sec, 4.56 km/sec and 4.96km/sec projectile velocity. The length and width of laminate was kept constant at 152.4mm and 101.6 mm in all cases. Each sample was pinned on its shorter edges as presented in Fig.12 [10]. The material of projectile is aluminium Al-2017 and Al 99.5% whereas its diameter is 0.8mm and 1.5mm. The results of experimental study are summarized in Table 3.

Experimental tests	Composite target		Projectile			Target damage	
Test Nr	Type	Thickness (mm)	Material	Diameter (mm)	Velocity (km/sec)	P/NP	Crater diameter Dc (mm)
6507	IM600/133	2,3	Al 2017	0,8	1,93	NP	1,13
6616		2,3		0,8	3,83	P	2,16
6588		2,3		0,8	4,56	P	2,02
6392		2,3	Al 99.5%	1,5	4,96	P	5,98

Table 3: Experimental test summary, NP and P means No-perforation and Perforation [10].

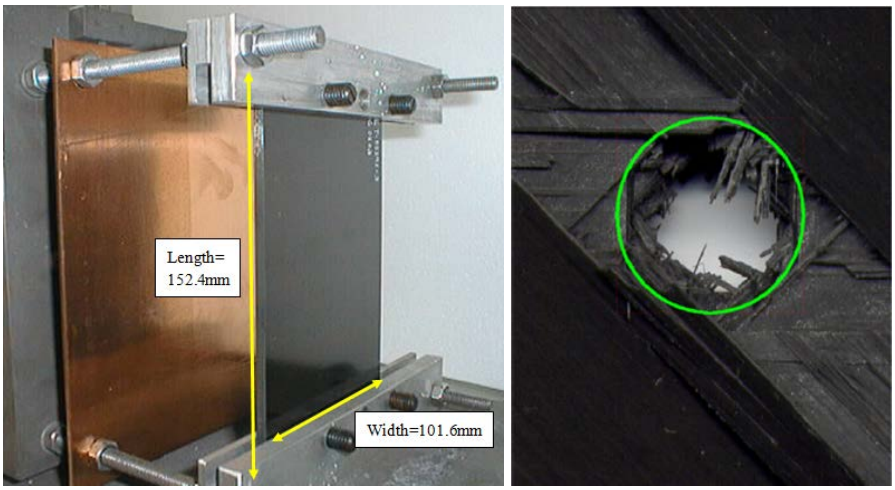

Fig.13: Left: Target mounting in the impact chamber. Projectile travels from right to left. Right: Crater diameter Dc [10].

6.2 Numerical simulation

The capture of ballistic limit and damage area constitute the main target of this study. For target attainment, the experimental tests Nr 6507, 6616 and 6588 were numerically represented. In particular, a hybrid model was generated using finite elements far away from impact point and particles near to this. The occupied circular area of SPH methodology has constant diameter 20 mm through the thickness. In both sections, ply-based composite modeling was adopted for the accurate representation of laminate structure instead of homogenized based one. The tying between finite elements and particles was achieved using the ***TIED_NODE_TO_SEGMENT** keyword. 552 particles with initial particle distance equal to 0.08mm were used for projectile modeling, whereas 62.856 particles were adopted for each ply modelling. The total number of particles of composite amounts to 1.005.696. In case of composite target, the initial particles distance was kept constant at 0.1mm in X and Y directions and 0.072 mm in Z direction.
The interaction between particles was defined using standard interpolation method (***CONTROL_CONT=0**) in case of particles into composite material and node to node contact interaction method between particles of projectile and target (***DEFINE_SPH_TO_SPH_COUPLING**). The penalty scale factor (**PFACT**) was supposed equal to 10. The **CLSH** parameter in ***SECTION_SPH** was proposed to be equal to 2 and the scale factor for minimum and maximum smoothing length was kept 0.1 and 4 respectively. In ***CONTROL** keyword, the renormalization approximation theory (**FORM=1**) was chosen since this theory provide the best results in previous verification section. Bucket sort based algorithm was used for smoothing length computation (**INI=0**), SPH particles were chosen to remain active (**IEROD=0**) and to be interact with others (**ICONT=0**) when failure criteria are satisfied. Concerning the boundary conditions, ***SPH_NODE_SET** and ***INITIAL_VELOCITY_GENERATION** were activated. The generated hybrid model is presented in Fig.14.

6.3 Results and Discussion

The results of simulations Nr 6507, 6616 and 6588 indicate that the ballistic limit of 2.3 mm thickness CFRP panel was captured accurately. When the velocity of projectile is 1.93 km/sec, no perforation exists and the experimental observation about peeling of rear face of laminate was verified. In case of 3.83 and 4.56 km/sec, all CFRP plies presented both fiber and matrix damage and the perforation of target is visible. The following screenshots justify the above conclusions. As far as the crater diameter is concerned, the Fig.16 shows the experimental and the numerical estimated diameter of damage. By the correlation of results, it is inferred that the SPH code is capable of capturing the extension of damage in a great extent.
For the evaluation of secondary debris distribution, the experimental test Nr 6392 was simulated. The experimental and numerical distributions of produced secondary debris during the phenomenon are presented in Fig.17. It is observed that the simulation does not capture the back scattered ejecta in first step and the cone of debris ejected rearward is not shown in second step of simulation. The detachment of superficial lamina and increased thickness around the impact crater are visible in both experiment and simulation.

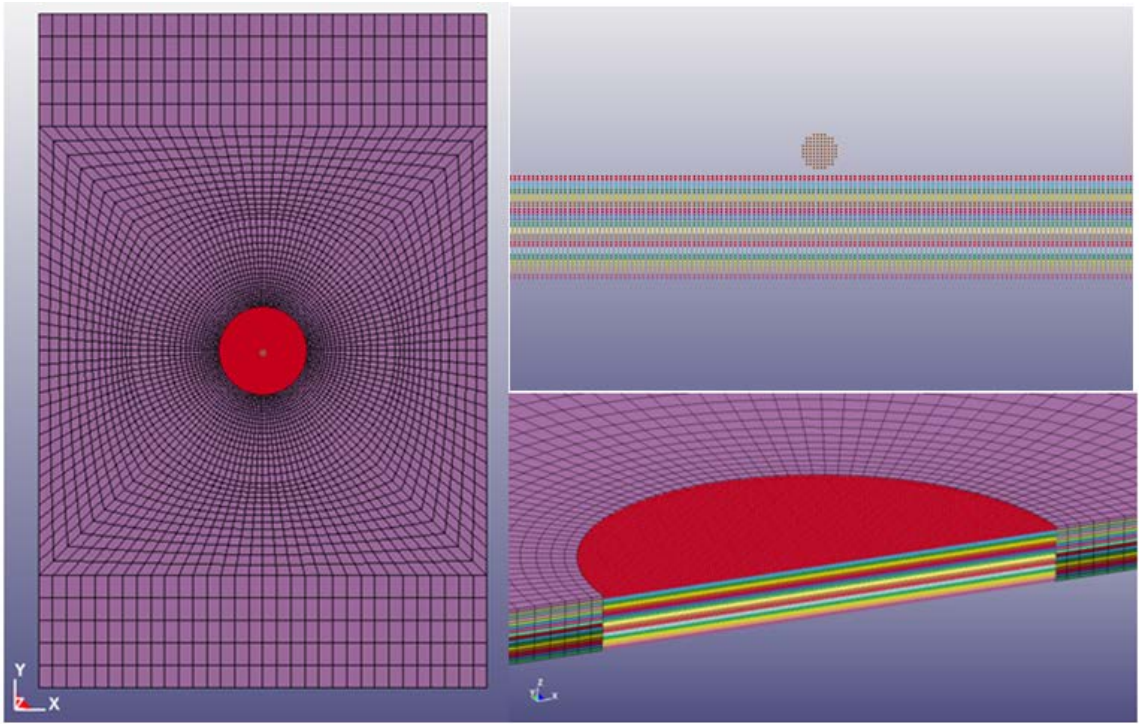

Fig.14: Hybrid FE-SPH model .

Simulation of Test Nr 6507 Velocity= **1.93** km/sec	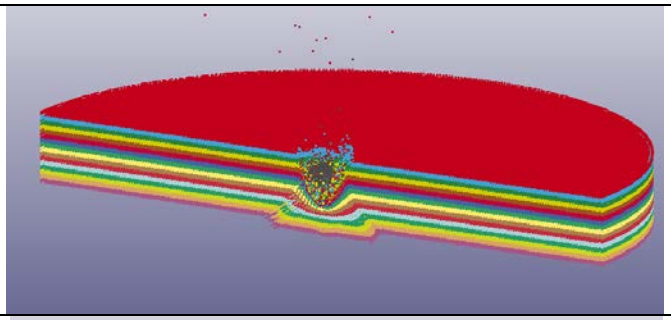
Simulation of Test Nr 6616 Velocity= **3.83** km/sec	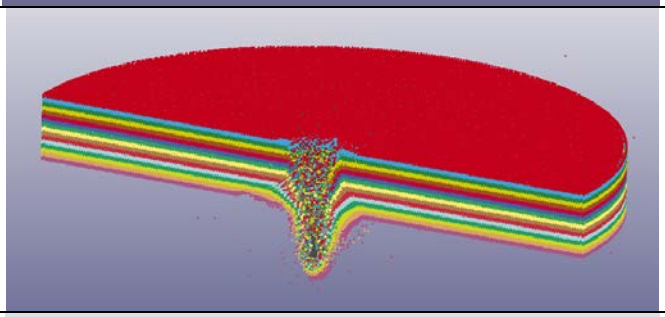
Simulation of Test Nr 6588 Velocity= **4.56** km/sec	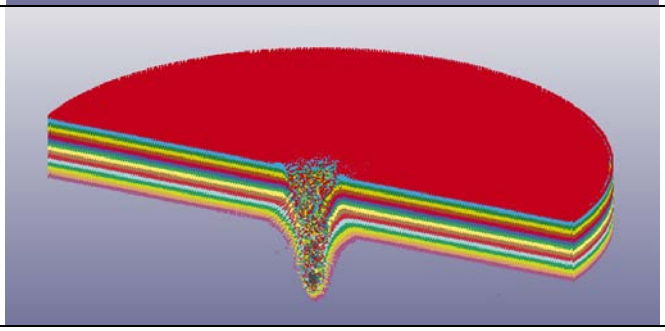

Fig.15: Hypervelocity impact responses of CFRP laminate for different projectile velocities.

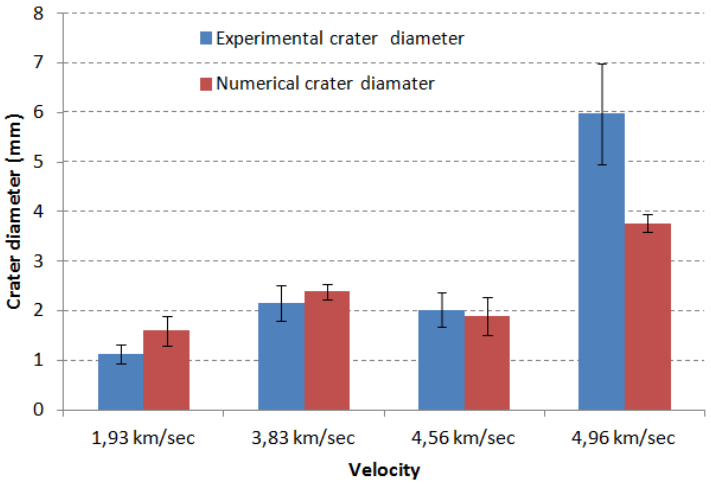

Fig.16: Comparison of experimental and numerical crater diameter.

Step	Experimental data [10] : Test nr.6392 (shadowgraphs)	Numerical simulation
1	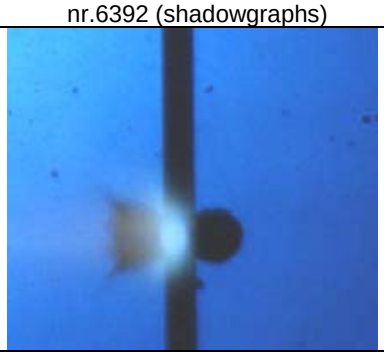	
2	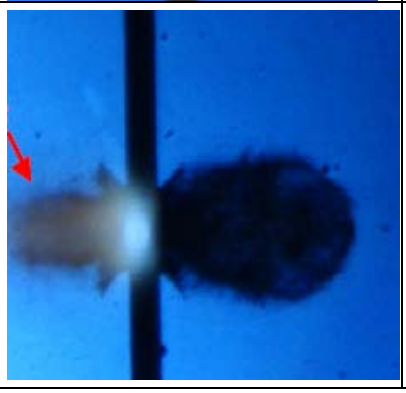	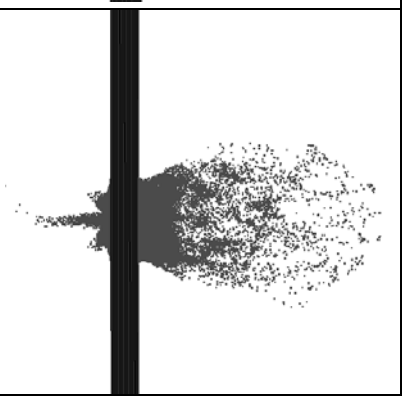

Fig.17: Experimental [10] and numerical ejecta distribution. Time delay between pictures is about 20μsec.

7 Summary

In current paper, the simulation of CFRP material behavior to hypervelocity impact using the smooth particle hydrodynamics (SPH) was studied. It was proved the verification of stiffness and failure of CFRP material to quasi-static level constitutes first-priority target when SPH methodology is applied, as SPH parameters play an important role to material response. It was indicated that the major SPH parameters which affect the material response are the particle approximation theory (FORM parameter) and the CLSH constant which applied to the smoothing length. Comparing theory and SPH methodology for different loadings, it was found that the numerical force-displacement curve is near to theoretical one when the renormalized approximation theory (FORM 1) is adopted and CLSH parameter was set equal to 2.

The HVI simulations showed that SPH code and MAT_59 provide reasonable results in view of the ballistic limit and the crater diameter of CFRP target plate after the verification of material response to quasi-static level. Concerning to secondary debris, further investigation in material properties, SPH

parameters and material models as well as additional experiments will be executed in order to evaluate if the LS-DYNA SPH methodology is capable of capturing the secondary debris phenomenon accurately. Additionally, in future, the influence of shock waves and strain rate effects on debris distribution should be assessed. Nevertheless, the presented work can serve as a useful reference for the modeling of composite materials behavior to HVI as their simulation using SPH methodology in LS-DYNA is limited.

Acknowledgments

The current work has been supported by the Horizon 2020 Program of the European Commission under the project: "Dynamic loading - Pushing the Boundaries of Aerospace Composite Material Structures" (EXTREME project).

8 Literature

[1] LS-DYNA® THEORY MANUAL, Livermore Software Technology Corporation.
[2] LS-DYNA® keyword user's manual R8.0, Livermore Software Technology Corporation.
[3] Xu, J., Wang, J.,: "Interaction methods for the SPH parts in LS-DYNA", 13th International LS-DYNA Users Conference.
[4] Lacome, L.J.,"SPH formulations: New Developments in LS-DYNA", 7th International LS-DYNA Users Conference.
[5] Hallquist, J., Cheng, W.,: "Implementation of three-dimensional Composite Failure Model into DYNA3D", retrieved from LSTC ftp server.
[6] Hara, E., Yokozeki, T., Hatta, H., Iwahori, Y., Ishikawa, T.,: "CFRP laminate out-of-plane tensile modulus determined by direct loading", Composites: Part A, vol 41, 2010, pp 1538-1544.
[7] Xiao, Y., Ishikama, T.,: " Bearing strength and failure behavior of bolted composite joints", Composites science and technology, vol 65, 2005, pp.1032-1043.
[8] Baluch, A.H., Park, Y., Kim, C.G,: High velocity impact characterization of Al alloys for oblique impacts", Acta Astronautica, vol.105, 2014, pp.128-135.
[9] Tiamiyu, A.A, Badmos, A.Y, Odeshi, A.G,: Effects of temper condition on high strain-rate deformation of AA 2017 aluminum alloy in compression", Material and Design, vol 89, 2016, pp 872-883.
[10] Francesconi, A., Giacomuzzo, C., Kibe, S., Nagao, Y., and Higashide, M.,: "Effects of high-speed impacts on CFRP plates for space applications", Advances in Space Research, vol. 50, 2012, pp. 539-548.